Power Handling Capability of Self-Resonant Structures for Wireless Power Transfer

Phyo Aung Kyaw, Aaron L. F. Stein and Charles R. Sullivan
Thayer School of Engineering at Dartmouth, Hanover, NH 03755, USA
{Phyo.A.Kyaw.TH, Aaron.L.Stein, Charles.R.Sullivan}@dartmouth.edu

***Abstract*—The range and efficiency of resonant inductive wireless power transfer depends on the quality factor of the resonant coils. A multilayer self-resonant structure (MSRS), made of many alternating layers of thin foil conductors and dielectric, has been shown to have a quality factor many times higher than conventional resonant coils of similar size. To date, the MSRS has only been modeled and tested for small-signal excitations and the impact of large-signal excitations on the MSRS performance has not been considered. This paper explores large-signal effects such as Steinmetz core loss, temperature dependence of winding and core losses, and the thermal effect of loss in order to determine the power handling capability of the MSRS. The analysis shows that a 6.6 cm-diameter prototype MSRS is capable of transferring as much as 10.7 kW over a 0.5 cm gap and 760 W over 2.2 cm, for maximum 40 °C temperature rise in a 25 °C environment.**

I. Introduction

The efficiency and achievable range of resonant inductive wireless power transfer (WPT) depend on the quality factor Q of the resonant coils and the magnetic coupling factor k between them. A large transmission distance, on the order of the resonant coil diameter, requires that the resonant coils have a high quality factor to compensate for the effect of low coupling between the coils. For shorter transmission distance, high Q can increase the efficiency, hence power handling capability [1].

Conventional WPT coils comprise a spiral of solid or litz wire placed on a ferrite magnetic core and connected to ceramic or film capacitors. In the kHz frequency range, litz wire is usually used to reduce the impact of skin and proximity effects which can significantly increase the winding loss. However, litz wire becomes increasingly cost prohibitive at MHz frequencies because the fine wire strands required for effective loss reduction are either too expensive or not commercially available. The high-current termination between litz wire and capacitors, and the electrode plate loss in the capacitors also contribute to losses in conventional WPT coils.

A multilayer self-resonant structure (MSRS), shown in Fig. 1, is an alternative resonant coil that overcomes many of the limitations of conventional WPT coils. It is made of C-shape conductive layers stacked in alternating orientations, separated by low-loss dielectric layers and placed in a magnetic core [2]. Equal current sharing among many thin conductive layers, achieved by capacitive ballasting, reduces proximity effect in the winding. The inductive coupling among foil conductors also eliminates resonant high-current terminations between the conventional coils and capacitors. The integrated capacitance provided by the dielectric layers eliminates the need for external capacitors, thereby eliminating the additional electrode plate loss in the capacitors. As a result, the MSRS provides a quality factor multiple times higher than conventional WPT coils of similar size; a prototype MSRS with a 6.6 cm diameter has a Q of 1173, more than 6 times higher than coils of similar size in the literature [3]. Thus, compared to conventional WPT coils, the MSRS can significantly improve range and efficiency of WPT and reduce the size of the resonant coils.

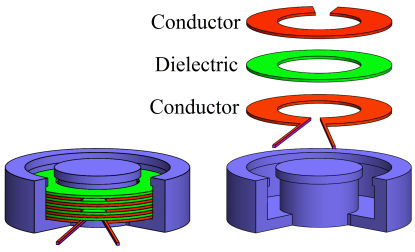

Fig. 1. Multilayer self-resonant structure with layer thickness exaggerated. Many layers, each on the order of 10 μm, are usually required in practice.

To date, the MSRS has been modeled and tested for small-signal excitations, and so its power handling capability has not been demonstrated. Although the small-signal loss models in [2]–[4] are valid in many low-power WPT applications, high-power applications may cause large-signal effects that have not been considered. For example, the complex permeability is not an accurate core loss model at high power levels; the large flux densities may require using the Steinmetz equation to calculate the large-signal core loss [5].

Moreover, there is a positive feedback loop between power losses in the resonant coils and the steady-state temperature. Losses in the structure cause temperature rise which can be significant for high power levels. This temperature rise in turn impacts the properties of materials used in the MSRS. The increase in conductor resistivity with temperature increases the dc resistance but lowers the proximity effect. The complex permeability and the Steinmetz parameters are also impacted by temperature rise. These changes in material properties with respect to temperature impact losses in the MSRS, which in turn affects the temperature rise, and so on.

This paper explores the impact of large-signal excitation

This work was supported by the National Science Foundation under Grant Number 1507773.

on the performance and temperature rise of the MSRS in order to determine its power handling capability. Other factors such as dielectric breakdown voltage (discussed in [6]) and health and safety considerations can also limit the achievable power capability. However, these factors are not considered in this paper and the analysis assumes that the dielectric layers are sufficiently thick to prevent dielectric breakdown and that human access to the coils is prevented.

A first-order thermal model is derived in Section II that relates losses in the MSRS to its temperature rise. The impacts of temperature on winding and core losses are discussed in Section III. A circuit model that represents a WPT system and an iterative algorithm used to find the equilibrium operating point are described in Section IV. The combination of these models allow for an examination of the effect of drive level and wireless range on the performance of the WPT system, and achievable power transfer level limited by a maximum tolerable temperature rise. Section V discusses the application of these models to a prototype MSRS as described in [4]; the analysis shows that a WPT system using a prototype MSRS with a 6.6 cm diameter, is capable of transferring as much as 10 kW over a 0.5 cm gap. Although the paper focuses on the MSRS, the presented models are also applicable to conventional WPT resonant coils and can be used with simple modifications.

II. Thermal Modeling

The achievable output power in a WPT system using the MSRS is limited by temperature rise due to losses in the resonant coils and the breakdown voltage of the dielectric layers. This paper assumes that dielectric layers of the MSRS are sufficiently thick so that breakdown voltage does not limit power handling capability; the impact of breakdown voltage on achievable output power is discussed in [6]. Because the power limit of the MSRS is constrained by the maximum operating temperature, it is important to model its thermal performance in order to examine the power capability.

The thermal model of the MSRS comprises resistance for conduction of heat generated inside the MSRS to the surface, and resistance for convection and radiation from the surface to the surroundings. For the MSRSs, and many WPT coils in general, the former can usually be ignored since the coils are usually thin and have a relatively large surface area. Appendix A verifies that the thermal resistance for internal conduction is negligible.

The thermal resistance for heat transfer from the MSRS surface to the surroundings $R_{th,\mathrm{amb}}$ comprises effects from both convection and radiation, and is given by

$$R_{th,\mathrm{amb}} = \frac{1}{h_{\mathrm{tot}} A} = \frac{1}{(h_{\mathrm{conv}} + h_{\mathrm{rad}})A}, \tag{1}$$

where h_{conv} and h_{rad} are heat transfer coefficients for convection and radiation respectively, h_{tot} the total heat transfer coefficient and A the MSRS surface area.

For natural convection in air, h_{conv} ranges from about 2 to 25 $\mathrm{W}/(\mathrm{m}^2 \cdot \mathrm{K})$ depending on the dimensions and orientation of the surface [7]. In this paper, we assume conservatively that $h_{\mathrm{conv}} \approx 8\ \mathrm{W}/(\mathrm{m}^2 \cdot \mathrm{K})$.

For radiation, the heat transfer rate is given by

$$\dot{Q} = \epsilon \sigma A (T^4 - T_a^4), \tag{2}$$

where ϵ is the emissivity of the surface material, σ Stefan-Boltzmann constant $\left(5.67 \times 10^{-8}\ \mathrm{W}/(\mathrm{m}^2 \cdot \mathrm{K}^4)\right)$, T the temperature of the MSRS surface in kelvin and T_a the ambient temperature in kelvin. The emissivity ϵ ranges from 0.85 to 0.89 for ferrite [8] and is around 0.9 for plastic [9]. Assuming that $\epsilon \approx 0.9$, the area specific heat transferred to the surroundings is 585 W/m^2 for 100 °C surface temperature in a 25 °C environment. Linearizing (2) for the 75 °C temperature rise gives a radiation coefficient of $h_{\mathrm{rad}} = 7.8\ \mathrm{W}/(\mathrm{m}^2 \cdot \mathrm{K})$.

Combining the effects of both convection and radiation, the total heat transfer coefficient to the environment is $h_{\mathrm{tot}} \approx 15.8\ \mathrm{W}/(\mathrm{m}^2 \cdot \mathrm{K})$. It should be noted that this heat transfer coefficient is an approximation and has a large uncertainty depending on surface geometry and orientation as well as ambient conditions.

III. Impact of High Power Levels on MSRS Losses

The MSRS's performance is impacted by losses in the winding, dielectric and magnetic core. Small-signal equivalent series resistances (ESR) representing these losses are modeled in [2], [3]. As the power level increases, nonlinear core loss properties and temperature rise can create losses in excess of that represented by the small-signal ESR. Such consequences of high power levels on winding and core losses are discussed in this section; the effect on dielectric loss is less significant since the low-loss dielectric materials such as polypropylene and PTFE are relatively stable with respect to temperature.

A. Impact on Winding Loss

Winding loss is impacted by power level due to the temperature dependence of resistivity ρ of metals, usually approximated as

$$\rho(T) = \rho_0 \left(1 + \alpha(T - T_0)\right), \tag{3}$$

where ρ_0 is the resistivity at a reference temperature T_0, and α is the temperature coefficient of resistivity. For copper, $\rho_0 = 1.68\ \mathrm{n\Omega \cdot m}$ at $T_0 = 20$ °C and $\alpha \approx 4 \times 10^{-3}\ \mathrm{K}^{-1}$ mean that the dc resistance of the winding at an operating temperature of 100 °C is approximately 32% higher than that at 20 °C. The ac resistance, however, increases by less than 32% because the higher resistivity increases the skin depth which in turn decreases the proximity effect among the conductor layers.

B. Impact on Core Loss

High power level impacts core loss by increasing the flux density inside the magnetic cores and or raising the temperature which in turns changes the properties of the magnetic material.

1) Impact of Flux Density: The core loss is calculated in [3] using the complex permeability model. This model is accurate for low flux densities but can significantly underestimate the core loss for high flux densities, at which the Steinmetz equation becomes more accurate for modeling the core loss. For a given flux density, the more accurate core loss model is the one that gives the higher loss [5].

The high Q of the MSRSs means that the current flowing into it, hence the induced magnetic flux density, is sinusoidal. Thus, the power loss per unit volume in magnetic core P_v according to the Steinmetz equation can be calculated as

$$P_v = k f^{\alpha} \hat{B}^{\beta}, \tag{4}$$

where $\hat{B}$ is the peak ac magnetic flux density, and k, α and β are Steinmetz parameters which are properties of magnetic materials and vary with the operating conditions [10]. Because the values of the Steinmetz parameters are frequency dependent, the core loss is sometimes characterized by

$$P_v = k_f \hat{B}^{\beta_f}, \tag{5}$$

where k_f and β_f are frequency dependent [11].

The peak ac flux density $\hat{B}$ depends on the transmission distance, the drive level and the core geometry, and is usually not uniform inside the pot core of the self-resonant structure. The core loss can be calculated by integrating the Steinmetz equation over the core volume using the local flux density at various points inside the core; this local flux density can be obtained by finite element analysis.

2) Impact of Temperature: Properties of the magnetic materials, such as the Steinmetz parameters and complex permeability, also depend on temperature. Manufacturers usually provide the Steinmetz loss data, the initial permeability and the temperature coefficient of the real part of the initial permeability for several temperatures. To the first order, the Steinmetz loss for an arbitrary temperature point can be interpolated using the available Steinmetz loss data. The temperature dependence of the imiginary permeability, however, is usually not provided and needs to be measured experimentally.

IV. Circuit Model for Wireless Power Transfer

A wireless power transfer system comprising two MSRS, or two coils with parallel resonance in general, and a load impedance can be modeled using the circuit shown in Fig. 2. Each resonant coil, on the first order, can be modeled as a parallel RLC circuit. The transmit coil is represented by the impedance Z_t, which is a parallel combination of L_t, C_t and R_t, and the receive coil by Z_r ($L_r \parallel C_r \parallel R_r$). The coupling between the two coils is described using a π-model consisting of three inductances L_t, L_r and L_{mid}, which can be obtained by magnetostatic finite element simulation. For a particular MSRS design, the capacitances C_t and C_r are independent of the power transfer distance x. The inductances L_t and L_r depend on magnetic coupling, hence on x. The resistances R_t and R_r, representing losses in the MSRS, depend on the power level, transmission distance and temperature as discussed in Section III.

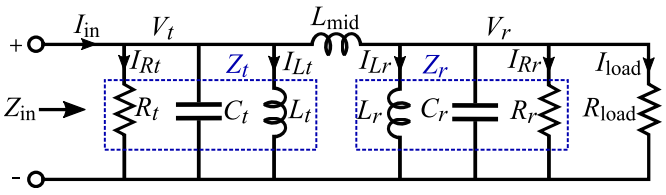

Fig. 2. Circuit model of a wireless power transfer system, using π-model for magnetic coupling. The impedance Z is the parallel combination of impedances due to the corresponding R, C and L.

For particular values of impedance in the circuit model, i.e. for two particular MSRSs separated by a particular distance operated at a specific power level, the loss fraction λ, defined as the ratio of power loss to the output power, is given by

$$\lambda = \frac{R_{\text{load}}}{R_r} + \frac{R_{\text{load}}}{R_t} \|H\|^2, \tag{6}$$

$$H = \frac{V_t}{V_r} = 1 + j\omega L_{\text{mid}} \left(\frac{1}{Z_r} + \frac{1}{R_{\text{load}}} \right), \tag{7}$$

where H is calculated by the voltage divider formula and detailed derivation of (6) is discussed in [6]. Minimizing λ in (6) with respect to R_{load} results in

$$\frac{1}{R_{\text{load,opt}}} = \sqrt{\frac{\Re\{H\}^2}{\omega^2 L_{\text{mid}}^2} + \frac{R_t}{\omega^2 L_{\text{mid}}^2 R_r} + \frac{1}{R_r^2}}, \tag{8}$$

$$\Re\{H\} = 1 + \frac{L_{\text{mid}}}{L_r} - \omega^2 L_{\text{mid}} C_r \tag{9}$$

where $\Re\{H\}$ is the real part of the voltage ratio H in (7). This $R_{\text{load,opt}}$ can then be used to calculate the theoretical maximum wireless power transfer efficiency, which in turn can be used, together with losses in the MSRS, to obtain the maximum output power for a given temperature rise.

A. Equilibrium Operating Point

The equilibrium operating point and temperature of a WPT system using two MSRSs can be obtained by considering the interdependence among power level, loss, temperature and optimal load resistance. For a particular WPT system including two MSRSs separated a certain distance apart, the inductances L_t, L_r and L_{mid} can be determined based on the core geometry and transmission distance while the capacitances C_t and C_r can be calculated from the winding geometry. All other circuit parameters, voltages and currents in the circuit, and the operating temperature are interdependent on each other. The various interdependences are summarized in Fig. 3.

This interdependence means that a transcendental equation would need to be solved to calculate the equilibrium operating point and temperature. Instead, the equilibrium operating point is obtained computationally using the following iterative process for each particular WPT system configuration, described by the geometry of the two MSRSs, the separation between them and the input current level.

1) Calculate L_t, L_r, L_{mid}, C_t and C_r based on the WPT system configuration.

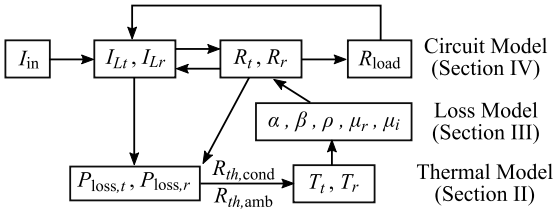

Fig. 3. Interdependence among various variables. The arrows show the direction of impact.

2) Calculate the small-signal ESR of the MSRSs using the loss models in [2], [3].
3) Choose the initial circuit parameters based on this small-signal ESR and an initial temperature of 25 °C.
4) Calculate $R_{\text{load,opt}}$ using (8).
5) Calculate power dissipated in the two WPT coils and the resulting temperature due to this dissipated power.
6) Perform finite element analysis to obtain the core loss using the Steinmetz equation.
7) Calculate core loss using the complex permeability model.
8) Update the circuit parameters using the larger of the core loss from the Steinmetz equation and the complex permeability model.
9) Repeat 4–8 until the temperature and the circuit parameters converge, or the temperature exceeds reasonable bounds.

Core loss data is typically only available up to 100 °C. Beyond that point, losses typically increase, and thermal runaway may occur. However, even if there are stable operating points above 100 °C, they are unlikely to be of practical value, so we do not attempt to extrapolate the core loss data or find those operating points.

V. Applying the Model to a MSRS Prototype

The thermal model in Section II, the loss model in Section III and the circuit model in Section IV are combined to calculate the power handling capability of a thin MSRS, whose design is discussed in [4]. The power capability is defined in this paper as the power output for a 40 °C temperature rise in a 25 °C environment.

A. MSRS Prototype

Fig. 4 shows the prototype MSRS, presented in [4], whose large-signal effects are quantified here. This coil comprises a 3.5 mm thick modified pot core of Fair-Rite 67 material with an outer diameter of $d = 6.6$ cm. Inside the pot core are 16 layers of 12.5 µm thick copper separated by 12.5 µm thick PTFE layers. The copper layers are C-shaped and stacked in alternating orientations.

Each of the two flat surfaces has an area of 34.2 cm^2. Using $h_{\text{tot}} \approx 15.8\ \text{W}/(\text{m}^2 \cdot \text{K})$ discussed in Section II, the thermal resistance for heat transfer from the MSRS surface to the ambient $R_{th,\text{amb}}$ is approximately 9.3 K/W. As discussed

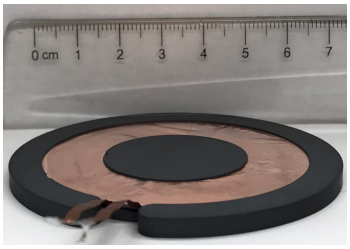

Fig. 4. The prototype MSRS [4].

TABLE I
Circuit Parameters of the Prototype MSRS. ESRs are calculated for small-signal excitation at 25 °C.

Parameter	Value	Comment
L	110 nH	Measured for a single MSRS.
C	5 nF	Measured for a single MSRS.
R_w	3.7 mΩ	Depends on T
R_{core}	1.6 mΩ	Depends on x, T and I_{in}
R_d	1.4 mΩ	Independent of x, T and I_{in}

in Appendix A, the thermal conduction resistance from inside the MSRS towards the surface can be ignored.

The prototype is characterized by inductance L, capacitance C and effective series resistances (ESR) representing losses in the winding R_w, the magnetic core R_{core} and the dielectric layers R_d, as shown in Table I. The inductance L and the capacitance C are obtained by impedance measurement of a single prototype MSRS. The ESRs in Table I are modeled as discussed in [3], [4], and the small-signal core ESR is calculated using the complex permeability model. The ESRs for higher drive levels and temperature need to be calculated using the thermal and loss models discussed in Sections II and III.

The temperature dependence of the Steinmetz loss is obtained from the data provided by the manufacturer. A comprehensive set of data is available only for 25 °C and 100 °C. The power loss data from the datasheet is interpolated to obtain the Steinmetz equations for 6.78 MHz operation: $P_v = 0.173\hat{B}^{2.784}$ for 25 °C and $P_v = 0.493\hat{B}^{2.605}$ for 100 °C where P_v is the volume specific power loss in mW/cm^3 and $\hat{B}$ the peak flux density in mT. The Steinmetz loss for an arbitrary temperature is obtained by linear interpolation of the Steinmetz losses for 25 °C and 100 °C. This linear interpolation is only approximate, but is sufficient for estimating the power capability of the MSRS for a maximum 40 °C temperature rise in a 25 °C environment.

The Fair-Rite datasheet provides information on the initial permeability and temperature coefficient for the real part of the initial permeability μ_r, but not the temperature coefficient of the imaginary permeability μ_i, which represents core loss. Thus, the impedance of a closed-core inductor with a 2-turn winding and a 67-material core was measured for several temperatures. The relative permeability was calculated from the measured impedance and is shown in Fig. 5; the core

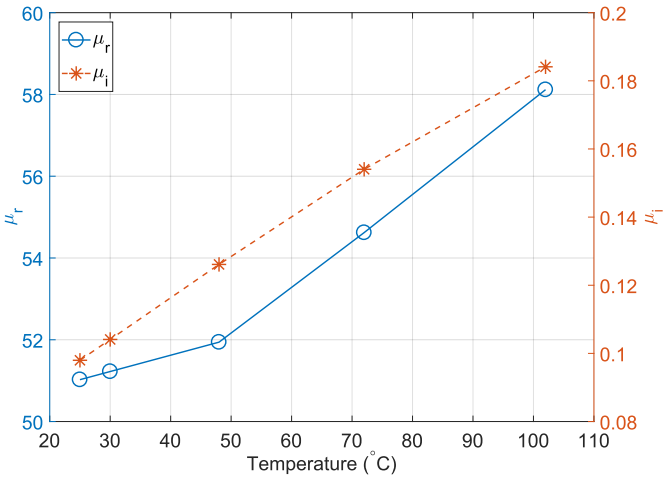

Fig. 5. Permeability of Fair-Rite 67 material vs. temperature, measured at 6.78 MHz using a pot core with an outer diameter of 6.6 cm and a closed-core height of 3.24 cm.

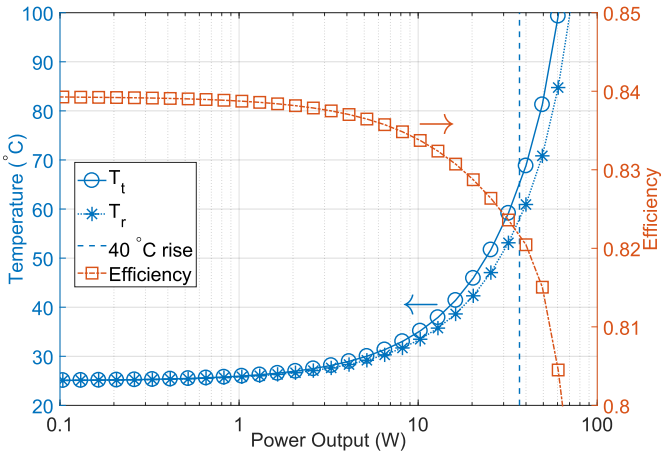

Fig. 6. Calculated equilibrium temperature and efficiency vs. output power for a WPT system comprising two of the prototype MSRSs separated 6.6 cm apart (= the coil diameter). The blue dashed line represents the 37 W power output corresponding to a 40 °C temperature rise in a 25 °C environment.

loss ESR for an arbitrary temperature point was calculated by interpolating μ_r and μ_i with respect to temperature.

B. Results

The effects of large-signal excitation was calculated for the prototype MSRS described above. For various power transfer distances and input current levels, the iterative process in Section IV-A was used to calculate the circuit parameters, losses and temperature at steady state.

Fig. 6 shows the results for a WPT system comprising two of the prototype MSRSs separated a distance $x = 6.6$ cm apart (equivalent to the diameter d of the prototype MSRSs). Up to about 1 W output, large-signal effects discussed in Section III are negligible; the equilibrium temperature for both coils remains around 25 °C and the WPT efficiency is about 84%. Large-signal effects become significant at around 5 W output. The receive coil temperature is lower than that of the transmit coil because the voltage induced in the recieve coil is lower than the voltage across the transmit coil, resulting in a lower power loss. The transmit coil temperature rises 40 °C for an output power of around 37 W. Higher power levels result in higher temperatures which is not useful for practical applications, and much higher power levels may cause thermal runaway in the MSRS, which can be predicted if core loss data are available for higher temperatures. However, such exercise may not provide much useful information for practical WPT coil designs.

This process was repeated for power transfer distance ranging from 0.5 cm to 13.2 cm ($x/d = 2$), and the result is shown in Fig. 7. Shorter power transfer distance results in higher magnetic coupling between the two resonant coils, hence higher WPT efficiency. Thus, for the same maximum tolerable temperature, i.e. for the same allowable power loss, much higher power can be transferred over a shorter distance. The analysis shows that the prototype MSRS is theoretically capable of transferring 10.7 kW over a 0.5 cm distance. For

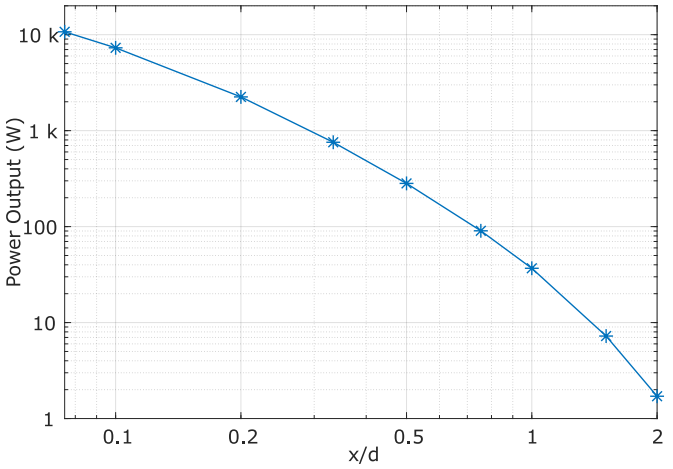

Fig. 7. Calculated maximum output power vs. wireless range normalized by the prototype MSRS coil diameter ($d = 6.6$ cm). The power is calculated for a 40 °C temperature rise in a 25 °C environment.

a distance of 13.2 cm, only about 1.7 W can be transferred because of very low magnetic coupling between the two coils.

It should be noted that the analysis ignores several factors which may impact the results. First, internal thermal conduction and heat transfer in the radial direction can be significant for MSRSs with thick magnetic cores such as the one discussed in [3]. Moreover, the mutual resistance of the winding is also ignored in this paper, which is approximately correct for weakly coupled coils. However, it can impact the MSRS loss for power transfer over a short distance. Finally, the total heat transfer coefficient $h_{\rm tot}$ was calculated assuming that heat can be transferred to the surroundings via both flat surfaces of each MSRS. However, for close-range power transfer, especially for the 0.5 cm, only one flat surface of each MSRS is available for heat transfer to the surroundings, which can significantly lower $h_{\rm tot}$. These factors can impact the results in Fig. 7, especially for shorter power transfer distances, and are topics for future research.

VI. Conclusion

A multilayer self-resonant structure is an alternative resonant coil which has been shown to have a small-signal quality factor multiple times higher than conventional resonant coils for wireless power transfer. This paper considered large-signal effects such as dependence of magnetic core loss on the drive level, temperature dependence of winding and core losses and the thermal effect of loss. The thermal, loss and circuit models presented in this paper can be used to estimate the power capability of the MSRS for various power transfer distances and output power levels. Even though the paper focuses on the large-signal effects for the MSRS, the analysis can be applied to conventional WPT coils with simple modifications.

The analysis shows that the prototype MSRS, with an outer diameter of 6.6 cm and a thickness of 3.5 mm, is capable of transferring up to about 760 W over a distance of 2.2 cm ($x/d = 1/3$) for a maximum temperature rise of 40 $^\circ\mathrm{C}$ in a 25 $^\circ\mathrm{C}$ environment. The power transfer capability is much higher for shorter transmission distance because of good magnetic coupling between the resonant coils; in theory, as much as 10.7 kW can be transferred over a 0.5 cm gap.

Future research work includes consideration of winding mutual resistance, more accurate thermal model for heat transfer from the surface to the surroundings, and experimental verification of the analysis. Health and safety limits may also constrain the allowable power levels and need to be considered in further research and development.

Appendix A
Verification of Negligible Conduction Resistance

The thermal resistance for conduction of heat generated inside the MSRS towards the surface is bounded from above by the thermal resistance for conduction from one flat surface of the MSRS to the other.

The MSRSs, and most WPT coils in general, are usually much thinner than wide. Thus, the majority of heat transfer from the MSRS to the surrounding is through the flat surfaces, and so a 1D thermal network model is sufficient to approximately describe the thermal conduction. Fig. 8 shows such a model including thermal conduction resistances of the core base $R_{th,b}$, the core center leg $R_{th,\mathrm{cen}}$, the core outer rim $R_{th,\mathrm{rim}}$ and the winding $R_{th,w}$. The thermal conduction resistance between the two flat surfaces is

$$R_{th,\mathrm{cond}} = R_{th,b} + (R_{th,\mathrm{cen}} \parallel R_{th,w} \parallel R_{th,\mathrm{rim}}). \qquad (10)$$

Thermal conduction resistance is given by $l/(kA)$ where l is the conduction length, A the conduction cross-sectional area and k the thermal conductivity. The resistances $R_{th,\mathrm{cen}}$, $R_{th,\mathrm{rim}}$ and $R_{th,b}$ can be calculated using appropriate values for l, k and A. In a MSRS, the winding is made up of alternating conductive and dielectric layers, resulting in

$$R_{th,w} = \frac{1}{\pi(r_{w,\mathrm{out}}^2 - r_{w,\mathrm{in}}^2)} \left(\frac{n_c t_c}{k_c} + \frac{n_d t_d}{k_d} \right), \qquad (11)$$

where n is the number of layers, t the layer thickness, k_c the thermal conductivity, $r_{w,\mathrm{out}}$ the winding outer radius and $r_{w,\mathrm{in}}$ the winding inner radius; the subscripts c and d represent the conductive layer and the dielectric layer respectively.

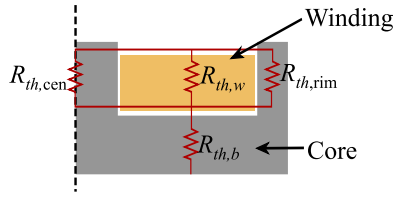

Fig. 8. Axisymmetric cross-section of the MSRS showing various thermal resistances. The figure is not drawn to scale; in practice, the thickness is much smaller than the radius. The winding (orange) is a stack of alternating C-shaped conductive layers separated by dielectric layers.

For the prototype MSRS (Section V-A), $R_{th,\mathrm{cond}} \approx 0.3\ \mathrm{K/W}$. Thus, thermal resistance for conduction of heat generated from inside the MSRS towards the surface is lower than 0.3 $\mathrm{K/W}$. Because $R_{th,\mathrm{amb}} \approx 9.3\ \mathrm{K/W}$, as much as 4.3 W can be transferred to the surroundings for a maximum temperature rise of 40 $^\circ\mathrm{C}$. Therefore, the temperature difference between the inside of the MSRS and the surface is at most 1.3 $^\circ\mathrm{C}$, and so the conduction thermal resistance can be ignored for a first-order thermal model.

References

[1] E. Waffenschmidt and T. Staring, "Limitation of inductive power transfer for consumer applications," in *13th European Conference on Power Electronics and Applications (EPE)*. IEEE, 2009, pp. 1–10.

[2] C. R. Sullivan and L. Beghou, "Design methodology for a high-Q self-resonant coil for medical and wireless-power applications," in *IEEE 14th Workshop on Control and Modeling for Power Electronics (COMPEL)*, 2013, pp. 1–8.

[3] A. L. F. Stein, P. A. Kyaw, and C. R. Sullivan, "High-Q self-resonant structure for wireless power transfer," in *32nd Annual IEEE Applied Power Electronics Conference and Exposition*, 2017, pp. 3723–3729.

[4] A. L. F. Stein, P. A. Kyaw, J. Feldman-Stein, and C. R. Sullivan, "Thin self-resonant structures with a high-Q for wireless power transfer," in *33rd Annual IEEE Applied Power Electronics Conference and Exposition (APEC)*, 2018, pp. 1–8.

[5] B. X. Foo, A. L. Stein, and C. R. Sullivan, "A step-by-step guide to extracting winding resistance from an impedance measurement," in *32nd Annual IEEE Applied Power Electronics Conference and Exposition (APEC)*, 2017, pp. 861–867.

[6] A. L. F. Stein, P. A. Kyaw, and C. R. Sullivan, "The feasibility of self-resonant structures in wireless power transfer applications," in *IEEE PELS Workshop on Emerging Technologies: Wireless Power (WoW)*, 2018, pp. 1–6.

[7] T. L. Bergman, A. S. Lavine, F. P. Incropera, and D. P. Dewitt, *Fundamentals of Heat and Mass Transfer*. John Wiley & Sons, 2011.

[8] Transmetra, "Table of emissivity of various surfaces," [Online] Available: https://transmetra.ch/images/transmetra_pdf/publikationen_literatur/pyrometrie-thermografie/emissivity_table.pdf, [Accessed Apr. 10, 2018].

[9] FLIR, "User's manual: FLIR Exx series," [Online] Available: https://www.flir.com/globalassets/imported-assets/document/flir-exx-bx-series-bx-user-manual.pdf, 2016, [Accessed Sep. 22, 2017].

[10] E. C. Snelling, *Soft ferrites: properties and applications*. Butterworths, 1988.

[11] A. J. Hanson, J. A. Belk, S. Lim, C. R. Sullivan, and D. J. Perreault, "Measurements and performance factor comparisons of magnetic materials at high frequency," *IEEE Transactions on Power Electronics*, vol. 31, no. 11, pp. 7909–7925, 2016.